EINDHOVEN UNIVERSITY OF TECHNOLOGY
Department of Mathematics and Computer Science

CASA-Report 10-59
October 2010

Modeling and optimization of algae growth

by

A. Thornton, T. Weinhart, O. Bokhove, B. Zhang, D.M. van der Sar, K. Kumar,
M. Pisarenco, M. Rudnaya, V. Savcenco, J. Rademacher, J. Zijlstra,
A. Szabelska, J. Zyprych, M. van der Schans, V. Timperio, F. Veerman

Centre for Analysis, Scientific computing and Applications
Department of Mathematics and Computer Science
Eindhoven University of Technology
P.O. Box 513
5600 MB Eindhoven, The Netherlands
ISSN: 0926-4507

Modeling and optimization of algae growth

Anthony Thornton, Thomas Weinhart & Onno Bokhove[*]

Bowen Zhang [†] Dick M. van der Sar [‡]

Kundan Kumar, Maxim Pisarenco, Maria Rudnaya, & Valeriu Savcenco [§]
Jens Rademacher & Julia Zijlstra [¶]

Alicja Szabelska & Joanna Zyprych[‖]

Martin van der Schans, Vincent Timperio & Frits Veerman [**] [††]

Abstract

The wastewater from greenhouses has a high amount of mineral contamination and an environmentally-friendly method of removal is to use algae to clean this runoff water. The algae consume the minerals as part of their growth process. In addition to cleaning the water, the created algal bio-mass has a variety of applications including production of bio-diesel, animal feed, products for pharmaceutical and cosmetic purposes, or it can even be used as a source of heating or electricity .

The aim of this paper is to develop a model of algae production and use this model to investigate how best to optimize algae farms to satisfy the dual goals of maximizing growth and removing mineral contaminants.

With this aim in mind the paper is split into five main sections. In the first a review of the biological literature is undertaken with the aim of determining what factors effect the growth of algae. The second section contains a review of exciting mathematical models from the literature, and for each model a steady-state analysis is performed. Moreover, for each model the strengths and weaknesses are discussed in detail. In the third section,

[*]Universiteit Twente 7500 AE Enschede, The Netherlands

[†]Delft University of Technology, 2628 CD Delft, The Netherlands

[‡]Phytocare, Noordeindseweg 58, 2651 CX, Berkel en Rodenrijs

[§]Technische Universiteit Eindhoven, P.O. Box 513, 5600 MB Eindhoven, The Netherlands

[¶]Centrum Wiskunde en Informatica. Department Modelling, Analysis and Computing. Science Park 123, 1098 XG Amsterdam, The Netherlands

[‖]Poznan University of Life Sciences, Wojska Polskiego 28, 60-637 , Poznan, Poland

[**]Leiden University, P.O. Box 9500, 2300 RA Leiden, The Netherlands

[††]Other participants: Amit Smotra, Katarzyna Marczynska & Vivi Rottschafer

a new two-stage model for algae production is proposed, careful estimation of parameters is undertaken and numerical solutions are presented. In the next section, a new one-dimensional spatial-temporal model is presented, numerically solved and optimization strategies are discussed. Finally, these elements are brought together and recommendations of how to continue are drawn.

KEYWORDS: Algae growth, steady-state analysis, parameter estimation, optimization.

1 Introduction

Greenhouses produce large amounts of mineral rich runoff water that needs to be treated to avoid ground-water contamination. The contaminants are mostly fertilisers such as nitrogen and phosphorus. It is both an environmental challenge and a legal requirement to avoid such contamination. A simple and efficient treatment to lower the nutrient concentration is to grow algae in shallow outdoor racetrack ponds, which are cheap and easy to maintain. This problem was presented by Phytocare who wants to achieve the following goals: To prove that algae cultures can clean runoff water; to obtain experience in growing algae cultures and develop protocols for industrial scale production; and to work toward producing an economically valuable product from the runoff water. This could be the start toward a new sustainable economic activity for greenhouse builders.

To grow algae, one requires not only nutrients but a supply of energy, which is provided by sunlight. The photosynthesis process converts photonic energy and carbon dioxide into glucose, or sugar. Thus, the pond requires an inflow of runoff water from the greenhouses as well as a pump that maintains a specified amount of carbon dioxide in the pool. The pond is continuously mixed to allow for homogeneous growth conditions and algae is continuously removed by 'sieving' the water, see figures 1 and 2.

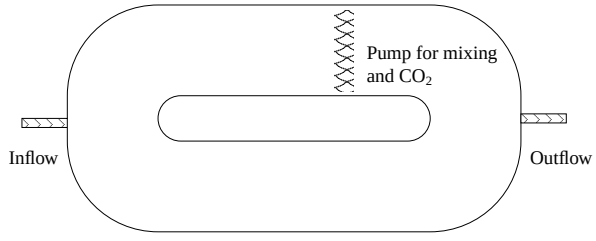

Figure 1: Schematic of a racetrack pond. Photos of the key parts can be seen in figure 2.

Algae not only remove the contaminates from water, but are an extremely important resource in many fields of industry. On the one hand, they can be employed for production of bio-diesel and bio-ethanol. On the other hand they form an important food source for shellfish or other animals. In addition, they are commercially cultivated for pharmaceutical and cosmetic purposes as well as to produce biomass, which is subsequently exploited to create heat and electricity. This wide variety of applications of algae explains the interest in controlling their growth.

The remainder of this paper is split into four sections. In the second second an hierarchy of exciting models from the literature is reviewed. For each model a equilibrium point analysis is undertaken and the limitations are discussed. In the third section a new two-stage ordinary differential equation model that considers the evolution of carbon, sugar, nutrients and algae is presented. Careful estimates for the parameters are obtained using a combination of the literature reviewed above and temporal averages of the equations. The fourth section presents an alternative partial differential equations model, which considers the depth and temporal evolution of two separate nutrients (phosphates and nitrates), carbon dioxide and algae growth. Numerical solutions are presented and a discussion of how to optimize the algae growth is undertaken. In the final section all these models and approaches are compared and contrasted, and then the factors that affect the growth of algae are discussed.

1.1 Brief review of existing literature

Before discussing mathematical models, we will briefly review some of the biological literature on the growth of algae; including a study of the conditions for optimizing the growth of algae and the removal of contaminants. We explain this process in terms of environmental conditions. The most important parameters regulating algal growth are temperature, nutrient quantity and quality, intensity of light, levels of CO_2 and O_2, pH and salinity. Knowledge about the influence and ranges of these parameters will help us to promote algae growth. The temperature of water as well as the nutrients content must be on the level that will allow the algae to grow [9]. The optimal temperature for phytoplankton cultures is generally between $20°C$ and $30°C$. Ranges for nutrients are presented in [12] and [6], whereas content of specific elements with focus on nitrogen and phosphorus is described in [15]. Since algae are photo-synthetic organisms, there is a need to set the cultures in areas of varying temperatures but with sufficient light to promote photosynthesis. Photosynthesis depends also on the light intensity and frequency. The photo-synthetic rate is proportional to irradiance and the higher the irradiance, the longer the dark period that can be afforded by the system without loss of growth

Figure 2: Images of an algae farm owned by Ingrepro: Top left, overview of the racetrack pond; top right, close up of the mixing device; bottom left, algae extraction apparatus; bottom right, bagged dry algae. Images reproduced with permission of Ingrepro, Borculo, The Netherlands. Website www.ingrepro.nl. Photos taken by V.R. Ambati.

[20]. Optimal light intensity for algae is 2,500-5,000 lux. According to Vonshak et al. [31], growth of algae becomes saturated at a range of $150 - 200 \mu mol$ photon $m^{-2}s^{-1}$. For a high photosynthesis rate balance between CO_2 and O_2 has to be taken into consideration [27]. In addition, Pulz in [27] described that species-specific O_2 evolution rates were recorded between 28 and 120 mg $O_2/(gDWh^{-1})$ in high-cell-density micro-algal cultures with optimum growth; whereas, Cheng *et al.* [6] studied the CO_2 concentration during algal growth and determined that the proper range is 0.8%-1.0%. Deviations from the optimum pH and salinity will cause productivity problems. Therefore optimum conditions should be maintained. The pH value for optimum growth of algae ranges between 7-12. Every algal species has a different optimum salinity range [4]. Paasche at al. [24] found a salinity range of 10 to 34 ppt for growth of clones of Emiliania huxleyi.

2 A hierarchy of models and some qualitative analysis

In this section we describe a hierarchy of increasingly complex, minimal models for light and nutrient limited algae growth which may serve as building blocks for more detailed models. All model ingredients were taken from the literature. The light-limitation is a crude model for the influence of photosynthesis on growth, lumped into a few parameters that would need to be gauged by measurements or extended by more detailed model components. This holds similarly for other influences, such as CO_2, pH value, etc. In the models presented in this section, we do not specify values for such parameters but rather investigate the qualitative dynamics of the algae growth and its interpretation.

We start with the purely light limited scalar model derived by Huisman *et al* in [12]. Inspired by the model in [10], see also [9], we extend this model by including two nutrients and a temperature dependence, but keep a scalar model. We then move on to a model by Klausmeier ([17, 16]) for nutrient-limited growth where nutrient densities are variable, and where intra- and extracellular densities are distinguished. Lastly, we combine this with the light-limitation model by Huisman ([12]).

2.1 The Huisman model: light-limited, nutrient surplus

This model has been derived in [12] and gives the density of algae $\mathcal{A}(t) \geq 0$ through the scalar ordinary differential equation

$$\frac{d}{dt}\mathcal{A} = \mathcal{H}(\mathcal{A}) := \overbrace{\frac{\mu_{\max}}{z_{\max}} \ln\left(\frac{H_P + I_{\text{in}}}{H_P + I_{\text{out}}}\right) \frac{\mathcal{A}}{k\mathcal{A} + K_{\text{bg}}}}^{\text{gain}} - \overbrace{h_r\mathcal{A} - D_r\mathcal{A}}^{\text{loss}}. \tag{1}$$

The parameters of the model can be roughly grouped into external, somewhat controllable, and internal, algae dependent parameters. All of these also depend to varying degrees on CO_2, pH value, temperature, nutrients, etc.

External parameters

incoming light:	I_{in}
outgoing light:	I_{out}
background turbidity:	K_{bg}
mixing depth:	$z_{\max}$
dilution / outflow:	h_r

Internal parameters

maximum specific growth rate:	$\mu_{\max}$
half saturation of photosynthesis:	H_P
specific light attenuation:	k
specific maintenance (death rate):	D_r

One of the main aspects of the model is that, even in the presence of mixing, the light intensity decays with depth due to 'shading' by algae above. For the above spatial average model this means:

$$I_{\text{out}} = I_{\text{in}} \exp(-(k\mathcal{A} + K_{\text{bg}})z_{\max}).$$

In [12] the form of the growth rate $\mathcal{H}$ is compared with ecological reality. For instance the inverse proportionality with respect to $z_{\max}$ suggests that shallow tanks are better for growth, which is well known in practice. Note that here this effect is given by a quantitative scaling law, and, for instance halving $z_{\max}$ has much greater effect than doubling I_{in}. We shall investigate some other qualitative predictions of this model.

Steady state analysis. The qualitative behaviour of a scalar ordinary differential equation is essentially determined by the location and stability of steady states, where $\mathcal{H}(\mathcal{A}) = 0$: the flow is monotone on intervals between equilibria with direction compatible with the (necessarily changing) stability of these equilibria. It is convenient to rewrite (1) in steady-state as

$$\mu_{\max} \ln\left(\frac{H_P + I_{\text{in}}}{H_P + I_{\text{out}}(\mathcal{A})}\right) = z_{\max}(k\mathcal{A} + K_{\text{bg}})(h_r + D_r), \tag{2}$$

where we divided by $\mathcal{A}$, to remove the trivial steady state $\mathcal{A} = 0$. The relative value of left and right hand sides (LHS, RHS) of this equation determines growth via

$$\frac{d}{dt}\mathcal{A} > 0 \Leftrightarrow \text{ LHS } > \text{ RHS}. \tag{3}$$

We first observe that LHS saturates for growing $\mathcal{A}$ to the asymptotic state $\mu_{\max} \ln\left(\frac{H_P+I_{\text{in}}}{H_P}\right)$, while RHS is growing linearly. This implies that for sufficiently large $\mathcal{A}$ we always have $\frac{d}{dt}\mathcal{A} < 0$ which makes intuitive sense as we expect that very large amounts of algae cannot be maintained.

Since the model is scalar, this decay can only be stopped by a steady state, which, in absence of positive steady states means $\mathcal{A} = 0$. The left and right hand sides at the state without algae satisfy:

LHS at $\mathcal{A} = 0$:

Value: $\mu_{\max} \ln\left(\frac{H_P+I_{\text{in}}}{H_P+I_{\text{in}}\exp(-K_{\text{bg}}z_{\max})}\right)$

Slope: $\mu_{\max} z_{\max} \frac{I_{\text{in}}\exp(-z_{\max}K_{\text{bg}})}{H_P+I_{\text{in}}\exp(-z_{\max}K_{\text{bg}})}$

RHS at $\mathcal{A} = 0$:

Value: $z_{\max}K_{\text{bg}}(h_r + D_r)$

Slope: $z_{\max}k\mathcal{A}(h_r + D_r)$

We infer that $\mathcal{A} = 0$ is the only steady state if the light intensity I_{in} is very small or if the depth $z_{\max}$ is very large. Again, this makes intuitive sense as 'life need light' to overcome depletion and natural death. The algebraic criterion for this

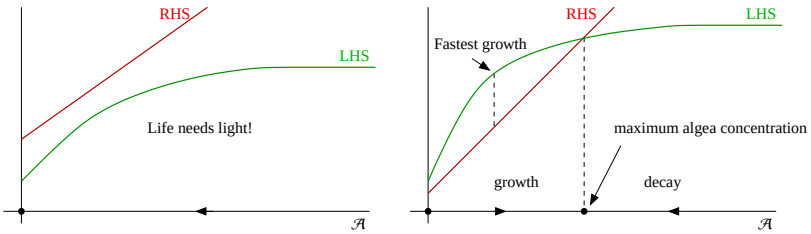

(a) (b)

Figure 3: Configurations without stable steady state (a) and mono-stability (b). Arrows on the horizontal $\mathcal{A}$-axis indicate the direction of growth. Bullets are steady states.

is cumbersome and does not provide much insight. A relatively simple sufficient criterion for the existence of another steady state above $\mathcal{A} = 0$ is that the value of LHS at $\mathcal{A} = 0$ is bigger than that of RHS:

$$\mu_{\max} \ln\left(\frac{H_P + I_{\text{in}}}{H_P + I_{\text{in}} \exp(-K_{\text{bg}} z_{\max})}\right) > z_{\max} K_{\text{bg}} (h_r + D_r). \tag{4}$$

As mentioned, this holds for large I_{in}, or for small $z_{\max}$ and K_{bg} i.e. a clean shallow tank, and can be somewhat controlled by small depletion (harvest) rate h_r.

Geometrically, steady states are intersection points of the graphs of LHS and RHS, see Figure 3. Since LHS is concave and RHS linear, under criterion (4) there is a single non-zero positive steady state. Since $\mathcal{A}$ larger than this implies decay as noted above, this steady state is stable, that is, when perturbing the amount of biomass the growth dynamics will be driven back to this state. This configuration may be called 'mono-stable' as the state without algae is unstable, which is ecologically perhaps unrealistic as it implies that even the smallest initial amount of algae suffices for stable growth up to a 'carrying capacity'. Note that the geometry implies that there is a single point of fastest growth, which means that a slowing of growth implies that the reactor is roughly halfway to its carrying capacity state.

The other possible configuration with positive carrying capacity is plotted in Figure 4. Here the initial amount of algae concentration has to lie above a threshold value to trigger growth until the carrying capacity state.

2.2 Huisman Model with nutrient limitation

As a first step to incorporate nutrient limitation we include a nutrient concentration dependent factor in the gain term, similar to the model in [10]. Denoting

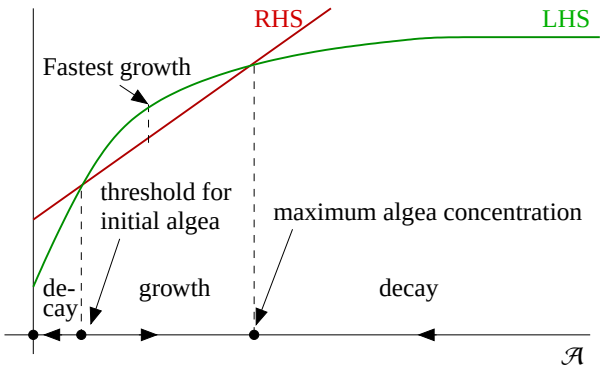

Figure 4: Typical dynamics of the Huisman model.

the amount of nitrogen and phosphorus as N and P, we assume for this factor the typical saturating form

$$\frac{P}{(H_P + \xi_P P)} \frac{N}{(H_N + N)}$$

known from generic growth models, where H_N, H_P are the half saturation parameters. To close the system, we assume instantaneous nutrient adaption

$$P = P_{\text{Tot}} - \alpha\mathcal{A}\,,\ N = N_{\text{Tot}} - \beta\mathcal{A},$$

where $P_{\text{Tot}}, N_{\text{Tot}}$ is the total influx of nutrients and α, β environmental parameters measuring the uptake into algae concentration.

It has been reported in the literature [5] that growth is more sensitive to Phosphorus, which we crudely model by taking the parameter $0 \le \xi_P < 1$. For simplicity, we initially set $\xi_P = 0$, so that the resulting model becomes invalid for large amount of P.

In addition, and mainly for illustration, we follow [10], see also [9], to include simple forms of temperature (T) dependence with respect to a reference temperature T_{ref} and rates θ_j, $j = 1, 2$.

$$\begin{aligned}\frac{d}{dt}\mathcal{A} \;=\; & \frac{\mu_{\max}}{z_{\max}} \ln\left(\frac{H_P + I_{\text{in}}}{H_P + I_{\text{out}}}\right) \frac{\mathcal{A}}{(k\mathcal{A} + K_{\text{bg}})} \\ & \times\theta_1^{T-T_{\text{ref}}} \frac{P}{(H_P + \xi_P P)} \frac{N}{(H_N + N)} \\ & -D\mathcal{A} - D_r\theta_2^{T-T_{\text{ref}}}\mathcal{A}.\end{aligned}$$

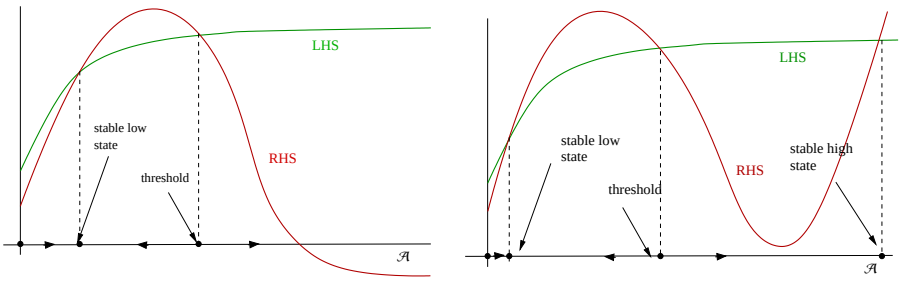

(a) (b)

Figure 5: Sketches of possible configurations for the extended Huisman model with nutrient limitation. (a) $\xi_P = 0$, (b) $0 > \xi_P \leq 1$.

Steady state analysis for $\xi_P = 0$. As above we pursue a steady state analysis and divide out $\mathcal{A} = 0$, which now gives

$$\frac{\mu_{\max}\theta_1^{T-T_{\text{Ref}}}}{z_{\max}\left(D + D_r\theta_2^{T-T_{\text{Ref}}}\right)} \ln\left(\frac{H_P + I_{\text{in}}}{H_P + I_{\text{out}}}\right) = \frac{(k\mathcal{A} + K_{\text{bg}})(H_N + N_{\text{Tot}} - \beta\mathcal{A})}{(P_{\text{Tot}} - \alpha\mathcal{A})(N_{\text{Tot}} - \beta\mathcal{A})}.$$

In essence, the left hand side is the same as in (2), but the right hand side is no longer affine. Instead, it has the shape sketched in Figure 5(a), and in particular has the negative asymptotic value $-k/\alpha$.

Therefore, large values of $\mathcal{A}$ imply $\frac{d}{dt}\mathcal{A} > 0$, which would mean unbounded growth. This is of course unrealistic, but as mentioned, the model becomes invalid for large values of $\mathcal{A}$. We infer that, within the range of validity, the largest steady state is always unstable, and may be $\mathcal{A} = 0$ in which case any initial amount of algae will grow (and eventually lie outside the range of validity).

The most interesting case is when there exists a positive *stable* 'low' steady state, which (to be consistent) implies the presence of a larger *unstable* 'threshold' steady state. This would mean that starting with initial algae below this larger unstable state and above any potential low threshold states, the reactor would always converge towards the low stable state. It would thus not reach its potential, which is an algae concentration so large that it is outside the range of this model.

One way to drive the reactor beyond the high threshold value would be control of the parameters, which is, however, beyond the scope of this article.

We note that it is for instance also possible that, geometrically, RHS lies below LHS everywhere, which implies unbounded growth for any amount of initial algae.

Steady state analysis for $0 < \xi_P < 1$. In this case the steady state equation reads

$$\frac{\mu_{\max}\theta_1^{T-T_{\mathrm{Ref}}}}{z_{\max}\left(D+D_r\theta_2^{T-T_{\mathrm{Ref}}}\right)}\ln\left(\frac{H_P+I_{\mathrm{in}}}{H_P+I_{\mathrm{out}}}\right)=\frac{(k\mathcal{A}+K_{\mathrm{bg}})(H_N+N_{\mathrm{Tot}}-\beta\mathcal{A})(H_P+P_{\mathrm{Tot}}-\alpha\mathcal{A})}{(P_{\mathrm{Tot}}-\alpha\mathcal{A})(N_{\mathrm{Tot}}-\beta\mathcal{A})}.$$

The main difference compared to $\xi_P = 0$ is that now the RHS asymptotically grows linearly, so that for large values of $\mathcal{A}$ we have the more realistic case $\frac{d}{dt}\mathcal{A} < 0$. As in the original model, this implies that the largest steady state is stable (which may be $\mathcal{A} = 0$). Qualitatively, and for small $\xi_P > 0$ also quantitatively, the discussion of $\xi_P = 0$ applies when augmented by a stable steady state larger than all others. This can be viewed as the 'carrying capacity' state of the reactor. In particular, the scenario of a stable low state now implies presence of a high stable state, which may be called 'bi-stability': coexistence of two stable states. Bi-stability is a signature of nonlinear systems and is analogous to a ball rolling in a landscape with two depressions: depending on the initial conditions, the ball can be caught in either and will remain there. In order to use the full potential of the reactor it is desirable to drive it always into the large carrying capacity state, but a discussion of this is beyond the scope of this short article. We only mention that a simple theoretical control would make the tank more shallow so that the maximum of RHS will be below the LHS curve.

We emphasize that local considerations near any fixed value of $\mathcal{A}$ cannot determine whether there exists such a larger stable state: It is an effect of global properties of the model. One indicator of bi-stability that uses medium-range deviation from a known potentially low stable state would be that the return towards this state significantly slows down upon increasing the perturbation in $\mathcal{A}$. This occurs when approaching the unstable threshold steady state between the low and high states: when the red and green curves get closer, the rate of decay becomes smaller, see Figure 5.

2.3 The Klausmeier model: nutrient-limited, light surplus

We describe the model from [17, 16] and summarize some relevant results. The model considers the biomass growth depending on the inner nutrient resources of the cells, rather than directly on the nutrient supply in the water. It thus accounts for limited physical space within the cells, which prevents uptake of arbitrary large quantities of raw nutrients, and the time it takes the cells to convert the raw nutrients into the biomass.

The nutrients available from the environment, R_N, R_P, corresponding to N and P, respectively, are thus distinguished from nutrients taken up from the water and stored within the algae cells, i.e., 'quota' nutrient: Q_N, Q_P. This approach also allows us to calculate the ratios of raw nutrients left in the water to the cell quota Q_i/R_i $(i = P, N)$.

Biologically meaningful initial conditions in this setting require $Q_i > Q_{\min,i}$, i.e., the cell growth starts only after a certain threshold value of stored nutrient has been surpassed. Furthermore, at the initial time $t = 0$ a certain amount of the biomass and nutrients are present in the water $\mathcal{A}(0) > 0$, $R_i(0) > 0$.

Klausmeier et al [17, 16] derived a 5-dimensional model, which describes the dynamics of the concentrations of two co-limiting nutrients and one algae species in an ideal chemostat (the nutrient supply rate a matches the algae dilution rate h_r).

$$\begin{aligned}
\frac{dR_i}{dt} &= a(R_{\text{in},i} - R_i) - \frac{v_{\max,i} R_i}{R_i + K_i}\mathcal{A} \\
\frac{dQ_i}{dt} &= \frac{v_{\max,i} R_i}{R_i + K_i} - \mu_{\max} \min_{j=1,2}\left(1 - \frac{Q_{\min,j}}{Q_j}\right) Q_i \\
\frac{d}{dt}\mathcal{A} &= \mu_{\max} \min_{j=1,2}\left(1 - \frac{Q_{\min,j}}{Q_j}\right)\mathcal{A} - h_r\mathcal{A}
\end{aligned}$$

The conservation law of this models concerns the total nutrients, which is given by $\sum_{j=1,2} R_j + Q_j\mathcal{A}$; note that Q_j is the nutrient concentration within a cell. Indeed, the rate of change of nutrients is equal to the nutrients added minus the nutrients removed from this system:

$$\frac{\mathrm{d}}{\mathrm{d}t}\sum_{j=1,2} R_j + Q_j\mathcal{A} = \sum_{j=1,2} a\left(R_{\text{in},j} - R_j\right) - h_r Q_j\mathcal{A}.$$

This model can easily be extended to the case of multiple species (e.g. [19]), competing for the shared resources, as well as incorporating the specific maintenance rate D_r. The latter is set to zero here: $D_r = 0$; the loss of algae is only due to washout from the chemostat.

In contrast to the previous scalar model, the dynamics of higher dimensional models are, in general, no longer determined by the location and stability of steady states alone. However, in this particular case it is: There is again the trivial steady state $\mathcal{A} = 0$, but also one nontrivial steady state, and if the latter exists, it is stable and the 'global attractor' [18] (all solutions with positive biomass converge to it). The nonzero steady state (if it exists) is thus the steady state carrying capacity.

For low initial amounts of nutrients, biomass evolution undergoes a number of stages. The first one is characterized by an 'exponential growth'-state, the so-called quasi-equilibrium state (where only biomass is not in equilibrium), during which the cellular quota ratio Q_N/Q_P matches the so-called *optimal* $N : P$ ratio $Q_{\min,N}/Q_{\min,P} = 27.7$, given in (mol N)/(mol P), which is also a condition for optimal growth [17, 16].

Thus, if the quota ratio Q_N/Q_P changes, it means that the exponential growth phase has been concluded and biomass has essentially reached equilibrium. If biomass production is the focus, one may increase depletion and harvest at this point. If the interest lies in water purification then the second stage is more interesting: the quota ratio Q_N/Q_P swings towards the supply ratio $R_{\text{in},N}/R_{\text{in},P}$ while the biomass is in equilibrium. This is because algae are, just as most living organisms, highly sensitive to their environment and able to adapt. Interestingly, the model also mirrors this feature and exhibits the flexibility of the cell quota being able to match the supply ratio at the optimal dilution rate of $h_r = 0.59\ \text{day}^{-1}$ [16]. These results have also independently been obtained in a series of chemostat experiments in [28, 29]. However, the harvesting of clean water should be done before the third stage starts, which is when the quota ratio falls back to the optimal ratio $Q_{\text{min},N}/Q_{\text{min},P}$ [16], and the biomass is still at equilibrium. Since the nutrient concentrations, the uptake rates and the quota are modelled separately, it is possible to determine the remaining concentrations of the nutrients in the water.

This model provides a fair description of phytoplankton/algae biomass growth and stoichiometry, which is determined not only by the nutrient supply stoichiometry in the chemostat, but also takes into account the physiological response of the algae.

2.4 Klausmeier-Huisman model: light and nutrient limited growth

The previous model is mainly focussed on the chemical resources, however, we know from the discussion of the scalar models, that light, i.e. energy, may be a limiting factor for algal biomass growth, so that the next logical step is to incorporate the light dependence.

The simplest extension in view of the discussion above would be the inclusion of the growth function in $\mathcal{H}$, see section 2.1, in the maximum growth rate $\mu_{\max}$, which then becomes

$$\frac{\mu_{\max}}{z_{\max}} \ln\left(\frac{H_P + I_{\text{in}}}{H_P + I_{\text{out}}}\right)/(k\mathcal{A} + K_{\text{bg}}).$$

The extended 'Klausmeier-Huisman' model thus reads, $i = 1, 2$,

$$\begin{aligned}
\frac{dR_i}{dt} &= a(R_{\text{in},i} - R_i) - \frac{v_{\max,i} R_i}{R_i + K_i}\mathcal{A} \\
\frac{dQ_i}{dt} &= \frac{v_{\max,i} R_i}{R_i + K_i} - \frac{\mu_{\max}}{z_{\max}(k\mathcal{A} + K_{\text{bg}})} \ln\left(\frac{H_P + I_{\text{in}}}{H_P + I_{\text{out}}}\right) \min_{j=1,2}\left(1 - \frac{Q_{\min,j}}{Q_j}\right) Q_i \\
\frac{d}{dt}\mathcal{A} &= \frac{\mu_{\max}}{z_{\max}(k\mathcal{A} + K_{\text{bg}})} \ln\left(\frac{H_P + I_{\text{in}}}{H_P + I_{\text{out}}}\right) \min_{j=1,2}\left(1 - \frac{Q_{\min,j}}{Q_j}\right)\mathcal{A} - h_r\mathcal{A}\,.
\end{aligned}$$

This still has the trivial steady state, and, depending on parameter values, possibly multiple nontrivial steady states. In that case the analysis of [18] fails. The criterion for stability of the trivial state is readily derived and reads

$$\Big(1 - \frac{\bar{Q}_{\text{lim, min}}}{\bar{Q}_{\text{lim}}}\Big)\frac{\mu_{\max}}{z_m K_{\text{bg}}} \ln\Big(\frac{H_P + I_{\text{in}}}{H_P + I_{\text{out}}}\Big) < h_r,$$

where $\bar{Q}_{\text{lim}}$ is the equilibrium value of the quota of the limiting nutrient (we omit the formula). For small dilution rate h_r this is violated, which means the trivial state would be unstable, the expected situation. Note that removing the light dependent part gives the analogous criterion for the above Klausmeier model, where instability of the trivial state implies that a non-trivial equilibrium is the global attractor. It would be interesting to find a natural connection (homotopy) from this to the scalar nutrient-limited Huisman model from section 2.2, and to analyze this model in more detail.

2.5 Conclusions

We reviewed selected minimal models and model building blocks for algae growth from the literature with focus on light and nutrient limitation effects. We showed a simple geometric way to interpret and understand the dynamics of the arising scalar models, in particular their carrying capacity states and the occurrence of bi-stability. Strategies for optimization are beyond the scope of this exposition, and would require better understanding of the actual values of parameters. In a nutshell, we claim that a qualitative analysis provides: consistency check, criteria for growth, estimates of growth rates and carrying capacity, and a framework for optimization. The next step would be to find realistic parameter values and to compare the result with real data.

In the final sections we briefly discussed a more realistic five dimensional model that includes nutrients as dynamic variables and distinguishes intra- and extracellular nutrient concentrations. We proposed an extension by the light-limitation building block of the previous models. Any satisfying mathematical analysis would require much more mathematical formalism and analysis. We refer to [18, 19] for studies in that direction.

3 An ODE model for algae growth

3.1 Mathematical model

In the previous section a hierarchical series of one-stage models was presented and a steady-state analysis undertaken, which revealed understanding of the long-term

behaviour of the pond. In this section a new two-stage model is presented and an attempted to obtain 'real' values for all the parameters that appear in the models is made. Due to the more complicated two-stage model a steady-state analysis is not performed, but the Huisman model (see section 2.1) can be obtained from a certain limit; therefore, the steady-state analysis could be used as test cases for the numerical solution presented at the end of this section. The derivation of this limit and numerical confirmation will not be covered in this publication.

Algae growth is a simple two-stage process, illustrated in Figure 6: carbon dioxide is pumped into the water and transformed into glucose by photosynthesis; then, nutrients provided by the drain water from the greenhouses and glucose combine to form new algae. Further, the algae, and the sugar stored in them, are assumed to be reduced by starving and harvesting. To keep the model simple, the nutrient composition is neglected, as well as the fact that energy can not only be stored in glucose, but also as more complex sugars and oils.

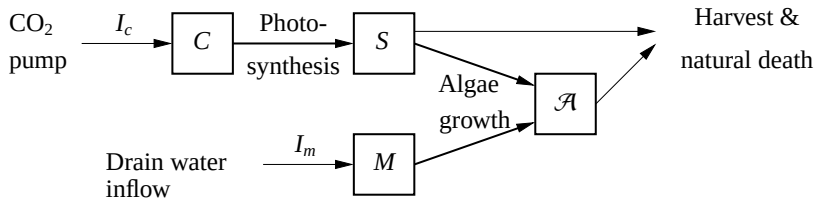

Figure 6: Production of algae from nutrients and carbon dioxide.

The algae production is modelled by the concentrations of dry algae $\mathcal{A}$, nutrients M, sugar S and carbon dioxide C in the pond. Assuming that the pond is well-mixed and algae growth is very slow, the above mentioned concentrations are independent of all spatial variables and only depend on time t; The inflow of nutrients and carbon dioxide into the pond is denoted by I_m and I_c, respectively. The algae are starving at a 'death rate' D_r and harvested at a rate h_r, both of which decrease the amount of algae and the sugar stored inside the algae. Further, sugar is produced at a rate $\alpha_s C$ from carbon dioxide, where α_s is the rate constant. This decreases the amount of carbon dioxide by a rate of $-k_1\alpha_s C$. From the oxygenic photo-synthetic process,

$$6CO_2 + 6H_2O \rightarrow (CH_2O)_6 + 6O_2,$$

we know that 44 g of carbon dioxide is needed to produce 30 g of sugar, yielding the conversion rate

$$k_1 = 44/30\ g[CO_2]\ g[(CH_2O)_6]^{-1}.$$

New algae are produced inside the existing algae at a rate $\alpha_{\mathcal{A}} N f_m(M)$ from nutrients and sugar, where $\alpha_{\mathcal{A}}$ is the rate constant and $f_m(M)$ denotes the concentration of nutrients inside the cells. This depletes nutrients and sugar by a rate of $-k_2\alpha_{\mathcal{A}} N f_m(M)$ and $-k_3\alpha_{\mathcal{A}} N f_m(M)$, respectively. Since mass has to be conserved, $k_2 + k_3 = 1$. Based on an estimate in [2] on the composition of algae,

$$k_2 = 0.1\,\frac{g[M]}{g[\mathcal{A}]}, \text{ and } k_3 = 0.9\,\frac{g[(CH_2O)_6]}{g[\mathcal{A}]}.$$

Units and a short description of all model parameters can be found in Table 1.

Combining the effects of algae growth, photosynthesis, inflow of carbon dioxide and minerals and starving and harvesting of algae, the following system of ODEs is obtained,

$$\dot{\mathcal{A}} = \alpha_{\mathcal{A}} f_m(M) S - (D_r + h_0)\mathcal{A}, \tag{5a}$$

$$\dot{M} = -k_2\alpha_{\mathcal{A}} f_m(M) S + I_m(t), \tag{5b}$$

$$\dot{S} = \alpha_s C - k_3\alpha_{\mathcal{A}} f_m(M) S - (D_r + h_0) S, \tag{5c}$$

$$\dot{C} = -k_1\alpha_s C + I_c(t). \tag{5d}$$

where the rate constants $\alpha_{\mathcal{A}} = \alpha_{\mathcal{A}}(\mathcal{A})$ and $\alpha_s = \alpha_s(\mathcal{A}, C, \lambda, \theta)$ are explained in section 3.2.

It should be noted, that in the current model we assumed the total amount of water is constant. We do not explicitly model the inflow/outflow of water or evaporation from the top of the pond . To fully treat the situation were the primary aim is to clean large volumes of run-off water an extra equation for the evolution of the total water volume is required. In the numerical examples presented below no clean water is removed from the system; therefore, this model is valid but additionally considerations are required to model the full decontamination problem.

Proper flux balance is obtained as the model obeys the following conservation law,

$$\frac{\mathrm{d}}{\mathrm{d}t}\left(\mathcal{A} + S + M + C/k_1\right) = -(D_r + h_r)(\mathcal{A} + S) + I_m + I_c/k_1, \tag{6}$$

One sees that the total mass involved is balanced by the nutrient and carbon dioxide input and the material lost by natural death and harvest.

3.2 Parameter values and functional dependencies

In the following section, we define the nutrient concentration inside the cell, $f_m(M)$, and the rate constants $\alpha_{\mathcal{A}}$ and α_S. All parameters used below are summarized in Table 2.

Par.	Unit	Description
$\mathcal{A}$	$g[\mathcal{A}]m^{-3}$	Concentration of dry algae
M	$g[M]m^{-3}$	Concentration of nutrients
$f_m(M)$	$g[M]m^{-3}$	Concentration of nutrients inside algae cells
S	$g[(CH_2O)_6]m^{-3}$	Concentration of glucose
C	$g[CO_2]m^{-3}$	Concentration of carbon dioxide
I_c	$g[CO_2]m^{-3}\text{day}^{-1}$	inflow of carbon dioxide
I_m	$g[M]m^{-3}\text{day}^{-1}$	inflow of nutrients
D_r	day^{-1}	(relative) algae death rate
h_0	day^{-1}	(relative) algae harvest rate
$\alpha_{\mathcal{A}}$	$g[\mathcal{A}]g[M]^{-1}g[(CH_2O)_6]^{-1}\text{day}^{-1}$	rate constant for biomass growth
α_s	$g[(CH_2O)_6]g[CO_2]^{-1}\text{day}^{-1}$	rate constant for photosynthesis
k_1	$44/30\ g[CO_2]\ g[(CH_2O)_6]^{-1}$	conversion rate of CO_2 into $(CH_2O)_6$
k_2	$0.1\ g[M]\ g[\mathcal{A}]^{-1}$	conversion rate of nutrients into dry algae
k_3	$0.9\ g[(CH_2O)_6]\ g[\mathcal{A}]^{-1}$	conversion rate of $(CH_2O)_6$ into dry algae

Table 1: Model parameters

We assume that the nutrient concentration inside the cell is saturated at $p_{max} = 0.4\ g[M]m^{-3}$ and that half-saturation is achieved when the outside nutrient concentration is $M_{turn} = 4\ g[M]m^{-3}$; thus,

$$f_m(M) = p_{max}\frac{M}{M + M_{turn}}. \tag{7}$$

The rate constants α_s, $\alpha_{\mathcal{A}}$ depend on various physical parameters. From [2], is it known that $\alpha_{\mathcal{A}}$ saturates with a increasing amount of algae and is half-saturated for $\mathcal{A}_{max} = 30g[\mathcal{A}]m^{-3}$, yielding

$$\alpha_{\mathcal{A}} = \alpha_{\mathcal{A}}(\mathcal{A}) = \hat{\alpha}_{\mathcal{A}} f_{\mathcal{A}}(\mathcal{A}), \text{ where } f_{\mathcal{A}}(\mathcal{A}) = \frac{\mathcal{A}}{1 + \mathcal{A}/\mathcal{A}_{max}}. \tag{8}$$

Further, the growth rate of algae is assumed to be proportional to the light intensity and further depends on the temperature and pH of the mixture. Therefore, α_s is proposed to have the following dependencies,

$$\alpha_s = \alpha_s(\mathcal{A}, C, \lambda, \theta) = \hat{\alpha}_s f_\lambda(\lambda, \mathcal{A}) f_\theta(\theta) f_{pH}(C), \tag{9a}$$

where f_λ, f_θ and f_{pH} model the dependence of the algae growth rate on light intensity, temperature and pH, respectively.

The photo-synthetic process in the algae depends on the light intensity and is therefore depth-dependent. However, since the pool is well mixed, the percentage

of light absorbed at any given depth is constant and the light intensity decreases exponentially. In [12], a depth-averaged light intensity is given by

$$f_\lambda(\lambda, \mathcal{A}) = \frac{a\mathcal{A}}{a\mathcal{A} + a_{bg}} \ln\left(\frac{H + \lambda}{H + \lambda e^{-(a\mathcal{A}+a_{bg})d}}\right), \tag{9b}$$

with λ the light intensity at the pond surface, pond depth $d = 30\ cm$, half-saturation constant H and light absorption constants of algae $a = 0.00455\ m^2 g[\mathcal{A}]^{-1}$ and background $a_{bg} = 7.2\ m^{-1}$ given in [12]. [1]

From [30], the photo synthesis rate is optimal at a temperature of $\theta_{opt} = 297\ K$ and vanishes at temperatures below $\theta_{min} = 269\ K$. This is modelled by a simple quadratic dependence,

$$f_\theta(\theta) = \max\left(0, 1 - \left(\frac{\theta - \theta_{opt}}{\theta_{min} - \theta_{opt}}\right)^2\right). \tag{9c}$$

We also know from the literature, see section 1.1 for a full discussion, that the photo-synthesis rate has an optimal pH level and does not grow in alkaline solutions. This optimum pH varies massively for different types of algae, here we take an optimal value of 7.4 (which is a little of the low side of the average, see section 1.1) and assume growth vanishes at at pH below 6.9. As shown in [22], pH does mainly depend on the amount of potassium and carbon dioxide. A typical potassium content was given in [3] to be 8 $g[KH]m^{-3}$. Thus, by [22], the minimal and optimal pH corresponds to a carbon dioxide content of $C_{max} = 24.9\ g[CO_2]m^{-3}$ and $C_{opt} = 7\ g[CO_2]m^{-3}$, respectively. This behaviour is modelled by a quadratic dependence,

$$f_{pH}(C) = \max\left(0, 1 - \left(\frac{C - C_{opt}}{C_{max} - C_{opt}}\right)^2\right). \tag{9d}$$

It remains to estimate the constants $\bar{\alpha}_s$, $\bar{\alpha}_{\mathcal{A}}$. Therefore we assume that the algae, nutrient, sugar and carbon dioxide concentrations are bounded; therefore, average values $\bar{\mathcal{A}}$, $\bar{M}$, $\bar{S}$, $\bar{C}$ exist, with $\bar{\cdot} = \lim_{T\to\infty} \frac{1}{T}\int_0^T \cdot\, dt$.

To estimate $\hat{\alpha}_{\mathcal{A}}$, we average equation (5b) over time $[0, T]$ and take the limit $T \to \infty$ to obtain

$$\lim_{T\to\infty} \frac{M(T) - M(0)}{T} = -k_2\hat{\alpha}_{\mathcal{A}}\overline{f_{\mathcal{A}}(\mathcal{A}) f_m(M)\S} + \bar{I}_m, \tag{10}$$

Since the nutrient concentration is bounded,

$$\lim \frac{M(T) - M(0)}{T} = 0;$$

[1] We note that the value given in [12] is $a = 0.7 \cdot 10^{-6}\ cm^2\text{cell}^{-1}$. From [21], we know that the maximal algae density is $5.6 - 7.5 \cdot 10^6$ cells ml^{-1} and 0.1 $g[\mathcal{A}]\ ml^{-1}$, from which we deduce that algae weigh about $1.5 \cdot 10^{-8} g\ \text{cell}^{-1}$.

therefore, we appoximate $\hat{\alpha}_{\mathcal{A}}$ by

$$\hat{\alpha}_{\mathcal{A}} \approx \frac{\bar{I_m}}{k_2 f_M(\bar{M})\bar{S} f_{\mathcal{A}}(\bar{\mathcal{A}})}, \tag{11}$$

where we assumed $\overline{f_M(M)S f_{\mathcal{A}}(\mathcal{A})} \approx \overline{f_M(M)S}\,\overline{f_{\mathcal{A}}(\mathcal{A})} \approx f_M(\bar{M})\bar{S} f_{\mathcal{A}}(\bar{\mathcal{A}})$, *i.e.*, the average of the total product equals the product of the average of each factor and the typical function value can be estimated by the function value at the typical parameter.

To estimate $\hat{\alpha}_S$, we average equations (5a)+(5b)+(5c) over time $[0, T]$ and take the limit $T \to \infty$ to obtain

$$\lim_{T\to\infty} \frac{(\mathcal{A} + M + S)|_0^T}{T} = \hat{\alpha}_S \overline{f_\lambda(\lambda, \mathcal{A}) f_\theta(\theta) f_{pH}(C) C} + \bar{I_m} - (D_r + h_r)(\bar{\mathcal{A}} + \bar{S}). \tag{12}$$

Assuming that the algae, mineral and sugar concentration is bounded, the left hand side of (12) vanishes; combining this with the fact that $\bar{C} \approx C_{\text{opt}}$ and $\bar{\theta} \approx \theta_{\text{opt}}$, we estimate $\hat{\alpha}_S$ by

$$\hat{\alpha}_S \approx \frac{(D_r + h_r)(\bar{\mathcal{A}} + \bar{S}) - \bar{I_m}}{f_\lambda(\bar{\lambda}, \bar{\mathcal{A}})\bar{C}}, \tag{13}$$

where we assumed as in (11) that

$$\overline{f_\lambda(\lambda, \mathcal{A}) f_\theta(\theta) f_{pH}(C) C} \approx \overline{f_\lambda(\lambda, \mathcal{A})}\;\overline{f_\theta(\theta)}\;\overline{f_{pH}(C) C} \approx f_\lambda(\bar{\lambda}, \bar{\mathcal{A}}) f_\theta(\bar{\theta}) f_{pH}(\bar{C}).$$

We estimate $\bar{\mathcal{A}}$, $\bar{C}$, $\bar{M}$, $\bar{S}$, $\bar{I_m}$, $\bar{\lambda}$, D_r and h_r by typical values from the literature:

- From [2], p. 36, a typical input rate of waste water is 7 to 20 $l\, m^{-3}$ day^{-1}. Assuming an average input of drain water of 20 $l\, m^{-3}$ day^{-1}, given a nitrogen concentration of 15 $m$mol$[N]l^{-1}$ and a molecular weight of 14$g$mol^{-1}, we estimate $\bar{I_m} = 4.2\; g[M]m^{-3}$day^{-1}.
- The input rate yields further that 2% of the water in the pool is changed per day, thus an order of magitude estimate is given by $\bar{M} = 2\% * \bar{I_m}$.
- The typical sugar content $\bar{S} = 10\; g[(CH_2O)_6]m^{-3}$ is an estimate from [3].
- Since the carbon dioxide input can be controlled, we assume $\bar{C} = C_{opt}$.
- A typical algae concentration was provided by [1] to be $\bar{\mathcal{A}} = 6\; g[\mathcal{A}]m^{-3}$.
- The typical light intensity on the surface is

  $$\bar{\lambda} = \lambda_{max}/2,$$

  where the maximum light intensity $\lambda_{max} = 2000\; \mu$mol photons m^{-2} is given by [23].

- The typical harvest rate is

$$h_r = \overline{h_r \mathcal{A}}/(\bar{\mathcal{A}} + \bar{S}),$$

  where a typical harvest of $\overline{h_r \mathcal{A}} = 12 g[\mathcal{A}] m^{-3} \text{day}^{-1}$ was given in [2].

- Finally, we use an estimate of the death rate $D_r = 0.46$ day^{-1} derived from [12].

Substituting these values into (13) and (11) we obtain

$$\begin{aligned} \hat{\alpha}_{\mathcal{A}} &\approx 102\ g[\mathcal{A}] g[M]^{-1} g[(CH_2O)_6]^{-1} \text{day}^{-1} \text{ and} \\ \hat{\alpha}_S &\approx 676\ g[(CH_2O)_6] g[CO_2]^{-1} \text{day}^{-1}. \end{aligned}$$

Param.	Value	Description	Source
p_{max}	0.4 $g[M]m^{-3}$	maximal nutrient concentration inside algae	
M_{turn}	4 $g[M]m^{-3}$	half-saturation constant for nutrient concentration inside algae	
$\mathcal{A}_{max}$	30 $g[\mathcal{A}]m^{-3}$	maximal algae concentration before growth shuts down	[2]
H	30 μmol photons m^{-2}	half-saturation constant	[12]
a	0.00455 $m^2 g[\mathcal{A}]^{-1}$	light absorption constant	[12, 21]
a_{bg}	7.2 m^{-1}	background light absorption constant	[12]
d	0.3 m	pond depth	
C_{max}	24.9 $g[\text{CO}_2]m^{-3}$	maximal CO_2 concentration for photosynthesis	[22, 3]
C_{opt}	7 $g[\text{CO}_2]m^{-3}$	optimal CO_2 concentration for photosynthesis	[22, 3]
θ_{min}	269 K	minimal temperature for algae growth	[30]
θ_{opt}	297 K	optimal temperature for algae growth	[30]
D_r	0.46 day^{-1}	algae death rate	[12]
h_r	2 day^{-1}	typical harvest rate	[2]
$\bar{\lambda}$	1000 μmol photons m^{-2}	average light intensity	[23]
$\bar{I}_m$	4.2 $g[M]m^{-3}\text{day}^{-1}$	typical nutrient inflow	[2]
$\bar{M}$	0.084 $g[M]m^{-3}$	typical nutrient concentration	$\bar{I}_m$
$\bar{C}$	7 $g[CO_2]m^{-3}$	typical carbon dioxide concentration	C_{opt}
$\bar{S}$	10 $g[(CH_2O)_6]m^{-3}$	typical sugar concentration	[3]
$\bar{\mathcal{A}}$	6 $g[\mathcal{A}]m^{-3}$	typical dry algae concentration	[1]

Table 2: Coefficients and typical values.

3.3 Limiting Behaviour and Threshold

The most well-known model for population growth is the logistic growth model. It appears naturally in models with one limiting resource. We describe in which way the system of ordinary differential equations (5) is related to a logistic growth model.

It is most natural to assume that the amount of minerals M is the limiting factor. We assume that the influx I_c is such that the CO_2-concentration is optimal, i.e. $\dot{C} = 0$. Since we only want the amount of minerals M to be a limiting factor, we should make differential equations (5a) for $\mathcal{A}$ and (5b) for M independent of S. We assume CO_2 is transformed into sugar very fast, i.e. α_s is very large. Now depending on the parameters in the model two things can happen: either α_s saturates at a large value of S, i.e. the photosynthesis will not become infinitely fast, or S itself saturates at a large value, i.e. the sugar reserve cannot become infinite. Both of these processes are not captured in the current model, since in the current model we assume S to be not too large. The second effect for example can be built in by replacing S in (5a), (5b) and the first S in (5c) by

$$f_S(S) := \frac{S}{1 + (1/S_{max})S}.$$

Furthermore, we assume $D_r = h_r = I_m = 0$, i.e. no natural death, harvest or inflow of minerals, and M and $\mathcal{A}$ are not too large. For M and $\mathcal{A}$ not too large $\alpha_{\mathcal{A}}$ behaves at leading order linear in $\mathcal{A}$: $\alpha_{\mathcal{A}} \sim \hat{\alpha}_{\mathcal{A}}\mathcal{A}$; similarly, f_m is at leading order given by

$$f_m \sim \frac{p_{max}}{M_{turn}} M.$$

Equations (5a) and (5b)reduce to

$$\dot{\mathcal{A}} = \hat{\alpha}_{\mathcal{A}} \frac{p_{max}}{M_{turn}} \bar{S} \mathcal{A} M, \tag{14a}$$

$$\dot{M} = -k_2 \hat{\alpha}_{\mathcal{A}} \frac{p_{max}}{M_{turn}} \bar{S} \mathcal{A} M, \tag{14b}$$

for some constant value $\bar{S}$. From these two equations it follows $\dot{M} = -k_2\dot{\mathcal{A}}$, thus $M(t) = M(0) + k_2\mathcal{A}(0) - k_2\mathcal{A}(t)$. Upon substitution in (14a) we obtain the logistic equation

$$\dot{\mathcal{A}} = \hat{\alpha}_{\mathcal{A}} \frac{p_{max}}{M_{turn}} \bar{S} \mathcal{A} \left(M(0) + k_2\mathcal{A}(0) - k_2\mathcal{A}(t)\right).$$

For certain parameter values a threshold for the growth process can emerge. The threshold manifests itself as an equilibrium in the $(\mathcal{A}, M, S, C)$ phase plane. Depending on the parameter values, this equilibrium can be stable. Acting as an

attractor, this would limit the growth of $\mathcal{A}$ to this equilibrium value. Taking the CO_2-input as the relevant bifurcation parameter, application of linear stability analysis at the equilibrium yields the result that for low I_c values, the equilibrium can indeed be stable.

3.4 Numerical Results

To investigate the behaviour of equations (5), the model was implemented in MATLAB. We first test the numerical model for the case of nutrient limited growth, as discussed in section 3.3. Thus, death rate, harvest rate and nutrient inflow is set to zero, I_c is chosen such that $\dot{C} = 0$ and temperature and CO_2 concentration is chosen to be at its optimal values θ_{opt}, C_{opt}, resp.. As initial values we choose

$$\mathcal{A}(0) = 3\, g[\mathcal{A}]m^{-3} << \mathcal{A}_{\max},\ M(0) = .4\, g[M]m^{-3} << M_{\text{turn}},\ \text{and}\ S(0) = 10\, g[S]m^{-3}.$$

The results of this simulation compares favorably with the analytic solution to the logistic limit equations (14), cf. Figure 7.

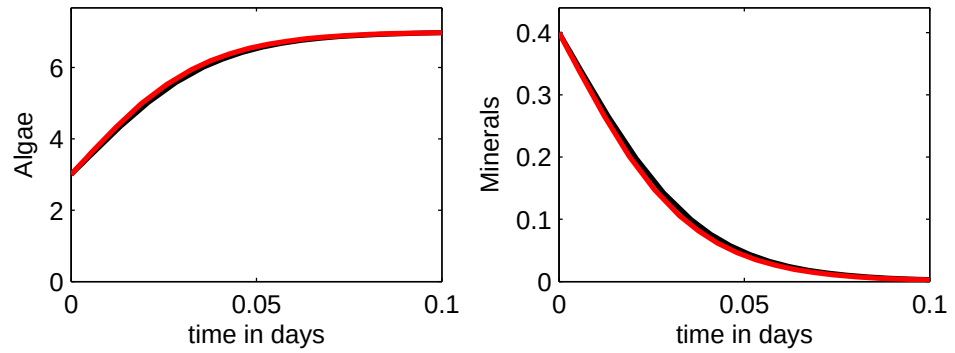

Figure 7: Comparison between results from the numerical model (black) and the logistic limit equations (red).

In the following we test the model for different parameter settings.

To optimize the photosynthesis process, the carbon dioxide inflow is controlled such that $C \approx C_{opt}$ by setting

$$I_c(t) = \beta \max(0\ g[C]m^{-3},\ C_{opt} - C),\ \beta = 4\ \text{day}^{-1}. \tag{15}$$

The ambient temperature was taken to be $\theta(t) = 293\ K$. To show that algae-growth can be nutrient-limited, we use a low nutrient influx of $I_m(t) = 0.2\, g[M]m^{-3}\text{day}^{-1}$. The simulation is started with a low algae concentration $\mathcal{A}(0) = 3g[\mathcal{A}]m^{-3}$ and

zero sugar, while we chose typical mineral and carbon dioxide concentrations $M(0) = \bar{M}$ and $C(0) = \bar{C}$. We evaluate on the time intervall $0 \leq t \leq 20$. We simulate three cases for different harvest and light intensity values, producing the results shown in Figure 8.

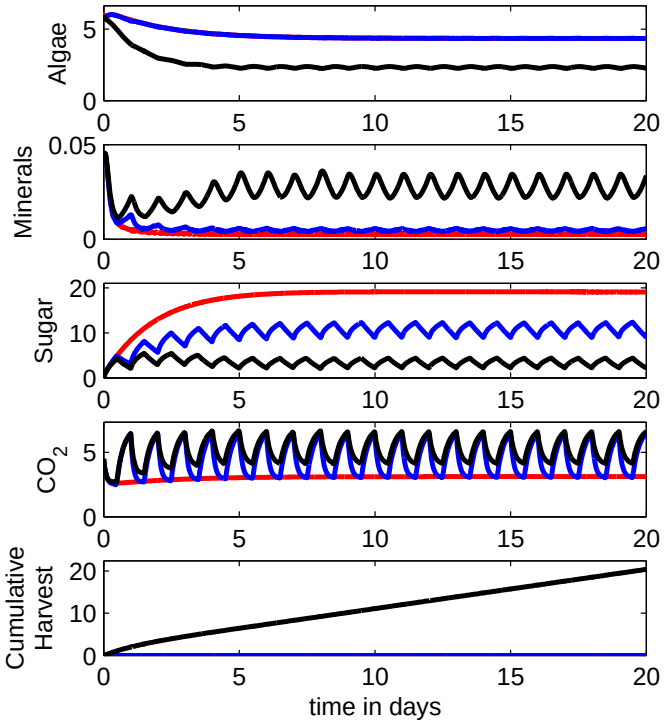

Figure 8: Concentrations for $t \in [0, 20]$. Red: $h_r = 0$ day^{-1}, $\lambda(t) = \bar{\lambda}$, blue: $h_r = 0$, $\lambda(t) = \lambda_0(1 + \text{sign}(\sin(2\pi t)))$, black: $h_r = 0.4$ day^{-1}, $\lambda(t) = \lambda_0(1 + \text{sign}(\sin(2\pi t)))$.

The red line shows the behaviour, when no harvesting is done and light intensity is constant,

$$h_0(t) = 0 \text{ day}^{-1}, \ \lambda(t) = \bar{\lambda}. \tag{16}$$

The algae grow rapidly until the nutrients are depleted. It then decreases towards a stable equilibrium, while the amount of sugar is increasing. Thus, the algae growth is nutrient-limited.

Next, a day-night cycle is modelled (blue line) by setting

$$h_0(t) = 0 \text{ day}^{-1}, \ \lambda(t) = \bar{\lambda}\,(1 + \text{sign}(\sin(2\pi t)))\,. \tag{17}$$

This decreases the amount of sugar, since the photosynthesis rate is non-linear w.r.t. the light intensity. Otherwise, this has only little effect on the algae growth, since it is nutrient- and not sugar-limited.

Finally, harvesting is turned on (black line),

$$h_0(t) = 0.4 \text{ day}^{-1}, \ \lambda(t) = \bar{\lambda}\,(1 + \text{sign}(\sin(2\pi t)))\,. \tag{18}$$

This significantly decreases the algae concentration. The mineral and sugar concentration now varies around a constant value with the day-night cycle. The mineral concentration initially decays in line with no harvest, but does not fall below a value of 0.2 [grams/m^3]. This would indicate that growing algae for harvest and removing most of the minerals from the water may be difficult in the same pond; therefore, a two coupled pond configuration, with one used to grow algae and the other to remove nutrients, maybe the only way to achieve the joint goal of nutrient removed and algae cultivation.

3.5 Conclusions

In this section a new two-stage model is presented: photo-synthesis converts the CO_2 to sugars and then minerals and sugar are combined to create new algal mass. If you take the limit of a quick photo-synthesis rate and a large bath of nutrients the original Huisman model §2.1 can be obtained. Additional in §3.4 it is shown that this two stage model can additionally be reduced to the logistic equation, when the only limiting factor is the supply of a single nutrient. Separating the minerals and modeling both phosphorus and nitrogen individually results in a system similar to the model studied in §2.2. In this fashion all the extra factors added in §2 can be added to this model and vice-versa.

Using parameter values from the literature and temporally averaged estimates, the equations were solved numerically. The effect of harvesting was studied and preliminary study seemed to suggest that two ponds would be best way to satisfy the dual goal of nutrient removal and algae growth.

In various sensible limits, this model can be reduced to the one-stage model presented in §2, which can be used to verify the numerical model and give insight into its behaviour in these limiting scenarios.

4 An alternative PDE Model

4.1 Mathematical Model

All the models considered in the previous sections are temporal models, they investigate the time-evolution of the total mass of algae in a given pond. In this section

a spatial-temporal model is presented that takes in account spatial depth variation within the ponds. Additionally, at the end of this section optimization of the model is discussed.

We study the growth of the algae (biomass) in the water body (described by the domain $\Omega \subset \mathbb{R}^3$). The biomass growth rate is related to the process of photosynthesis, the process of mixing and the death rate. The process of photosynthesis depends upon the concentration of the nutrients, the availability of CO_2 and the availability of light. The death rate includes both the harvesting rate as well as the natural death rate of the algae. Since the light intensity is uneven at different depth of the water body, it is important to stir the water to mix the algae. Advection is assumed to be absent which corresponds to the still water body. In the horizontal plane, we consider no variation and hence, the growth rate is independent of x and y coordinates. The depth in the water body is denoted by z.

The growth rate of the algae biomass is given by

$$\partial_t \mathcal{A} = g(I_{\text{in}})\, f_1(P)\, f_2(N)\, f_3(C)\mathcal{A} + D_M \partial_{zz}\mathcal{A} - H_a(\mathcal{A}). \tag{19}$$

The mixing is modeled by a diffusion term with a constant coefficient D_M. Inclusion of the mixing term helps to understand the effect of mixing on the overall production rate of the algae. The functions $g(I_{\text{in}})$, $f_1(P), f_2(N)$ and $f_3(C)$ define the dependence of the biomass growth rate on the light intensity, the concentration of nutrients (phosphates and the nitrates), and the carbon dioxide. Function $H_a = (h_r + D_r)\,\mathcal{A}$ describes the death rate of the algae biomass including both the harvesting term as well as the natural decay rate. A similar model was used in [13, 25]. For the light intensity, we take the Monod form of dependence [11]

$$g(I_{\text{in}}) = \frac{\mu_0 I_{\text{in}}}{H_L + I_{\text{in}}}, \tag{20}$$

where I_{in} is the effective light intensity received by the algae and H_L is the half saturation intensity. The Monod form ensures that the growth rate is almost linear when the light intensity is very small, and the growth rate remains bounded by μ_0 when I_{in} becomes very large. The light intensity received by the algae is not uniform throughout the water body. The light intensity is attenuated by two factors: the presence of algae and the water mass. The presence of the algae in the top layers causes reduction in the available light for the algae in the deeper layers. This describes the non-transparency of the water body due to the presence of algae. Moreover, the water layers themselves cause attenuation in the available light intensity for the deeper layers. In the light of the above discussion, the light intensity can be modeled by

$$I_{\text{in}}(z,t) = I_0(t) e^{-kz} e^{K(z)} \tag{21}$$

where

$$K(z) = -r_s \int_0^z \mathcal{A} dz$$

where $I_0(t)$ is the incident light intensity which changes in time (for instance during the day and night cycle). The constant k is the specific light attenuation coefficient due to the water layer and r_s is the specific light attenuation coefficient due to the presence of algae.

For the nutrients, the phosphates and the nitrates, we once again take the Monod type rates

$$f_1(P) = \frac{k_P[P - P_c]_+}{H_P + [P - P_c]_+}, \tag{22}$$

$$f_2(N) = \frac{k_N[N - N_c]_+}{H_N + [N - N_c]_+}. \tag{23}$$

Again, H_P and H_N are the half saturation concentrations of phosphorus and nitrates respectively. The $[\cdot]_+$ denotes the positive cut-off function $[x]_+ = \max(0, x)$. Parameters P_c and N_c are the critical concentration of the nitrates and phosphates, respectively, below which the growth becomes zero. To model the effect of CO_2 we note that the presence of carbon dioxide affects the pH value of the water. We assume for simplicity that pH value is solely determined by the presence of the CO_2. The growth rate of the algae is influenced by the pH value apart from the other factors that we discussed above. The consumption of CO_2 leads to the reduction in the CO_2 concentration and hence, leads to the increase in pH value. It is known that there is a certain range of pH value where the algae growth is optimal. Hence, if the source of CO_2 provides more than required, the pH value of the water body will decrease. This decrease can lead to the enhancement of the death rate of the algae. The growth rate dependence is modeled by the functional form that monotonically decreases with pH (and hence monotonically increasing with the concentration of CO_2) however, at higher concentrations of CO_2 the growth rate becomes constant and bounded. We consider the following functional form

$$f_3(C) = \frac{1}{1 + e^{\lambda\left(pH(C) - pH_{opt}\right)}}, \tag{24}$$

where λ is a parameter that describes the sharpness of the profile and pH_{opt} describes the 'switching' value of pH at which the growth increases if all other factors are kept unchanged. The relation between the pH and CO_2 is given as

$$pH(C) = (6.35 - \log_{10} C)/2.$$

This relation is obtained using the chemical equilibrium constant of the hydrolysis of the carboxylic acid. The modeling of the harvesting term includes the specific

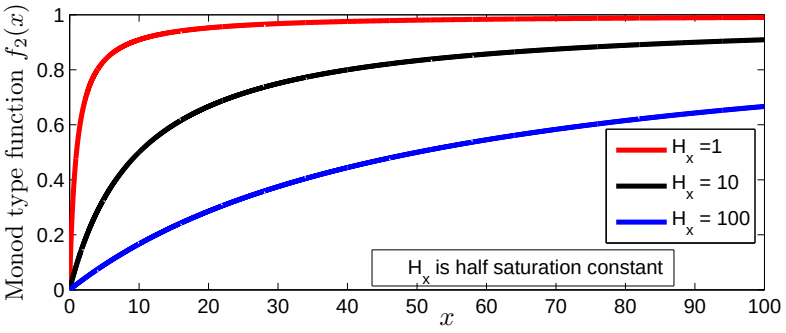

Figure 9: Monod type function for different half-saturation constants.

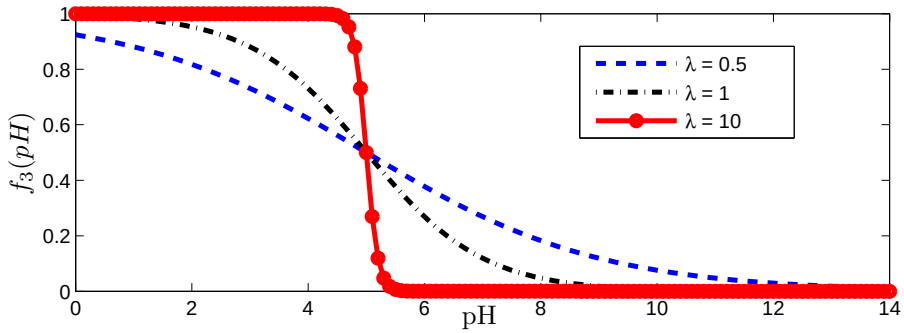

Figure 10: $f_3(pH)$ function for different values of parameter λ.

death rate having pH dependence so that at small pH the death rate enhances. We propose the following functional dependence for this term similar to the $f_3(pH)$

$$H_a(w) = D_r\, f_4(C)\mathcal{A}\,, \tag{25}$$

with

$$f_4(C) = \frac{1}{1 + e^{\lambda\left(pH(C) - pH_{dopt}\right)}}\,, \tag{26}$$

where pH_{dopt} is again the 'switching' value of the pH at which the death rate increases. In Figure 9 and Figure 10 we illustrate the nature of Monod- and f_3 functions.

We complete the system with the following ordinary differential equations de-

scribing the evolution of the nutrients and the CO_2

$$\begin{aligned}
\frac{dN}{dt} &= -\frac{1}{z_{\max}}\left(\int_0^{z_{\max}} g(I_{\text{in}})f_1(P)f_2(N)f_3(C)\mathcal{A}dz\right)N + S_N,\\
\frac{dP}{dt} &= -\frac{1}{z_{\max}}\left(\int_0^{z_{\max}} g(I_{\text{in}})f_1(P)f_2(N)f_3(C)\mathcal{A}dz\right)P + S_P,\\
\frac{dC}{dt} &= -\frac{1}{z_{\max}}\left(\int_0^{z_{\max}} g(I_{\text{in}})f_1(P)f_2(N)f_3(C)\mathcal{A}dz\right)C + S_C,
\end{aligned} \tag{27}$$

where $z_{\max}$ is the maximum depth of the water body.

We use homogeneous Neumann boundary conditions for (19) and we require the following initial conditions

$$N(0) = N_0, \quad P(0) = P_0, \quad C(0) = C_0, \quad w(z,0) = w_0(z). \tag{28}$$

Equations (19), (27) together with initial conditions (28) constitute the system of equations under study. We use the following values of the parameters for the numerical computations taken from [8, 11, 10].

$\mu_0 k_p k_N[1/s]$	$H_L[W/(m^2 \cdot day)]$	$H_N[g/l]$	$H_P[g/l]$
0.0886	70	$14.5 \cdot 10^{-6}$	$10.4 \cdot 10^{-6}$

$r_s[l \cdot m/g]$	$k[1/m]$	$D_M[m^2/s]$	$D_r[g/(l \cdot day)]$
10	0.2	$5 \cdot 10^{-4}$	0

The values of the parameters chosen are realistic, however, not all the parameters are exactly known and approximate values are taken for those parameters. The model is generic and for a given type of algae these parameters need to be determined experimentally. Here, we need the parameters to see whether the obtained results are realistic.

4.2 Numerical experiment

In this section we test our model for the set of parameters presented in the previous section. We solve the system (19),(27)-(28) using the method of lines (MOL) approach which consists of two stages. The first stage is the spatial discretization in which the spatial derivatives of the PDE are discretized, for example with finite differences, finite volumes or finite element schemes. By discretizing the spatial operators, the PDE with its boundary conditions is converted into a system of ODEs in $\mathbb{R}^m$

$$\boldsymbol{W}'(t) = \boldsymbol{F}(t, \boldsymbol{W}(t)), \quad \boldsymbol{W}(0) = \boldsymbol{W}_0, \tag{29}$$

called the semi-discrete system. This ODE system is still continuous in time and needs to be integrated. So, the second stage in the numerical solution is the numerical time integration of system (29).

We discretize the diffusion operator in (19) by standard second-order central differences on a fixed uniform grid $0 = z_1 < z_2 < \ldots < z_m = z_{max}$. The integral term within the light function (21) is approximated by

$$\int_0^{z_k} \mathcal{A} dz_k \approx \frac{z_k}{k} \sum_{i=1}^{k} z_i \, .$$

The other integral term used in (27) is approximated by

$$\int_0^{z_{\max}} g(I_{\text{in}}) f_1(P) f_2(N) f_3(C) \mathcal{A} dz \approx \frac{z_{\max}}{m} f_1(P) f_2(N) f_3(C) \sum_{i=1}^{m} g(I_{\text{in}}(z_i, t)) z_i \, .$$

The obtained system (29) is stiff due to the diffusion term, therefore, an implicit numerical integration method must be used. We use the two-stage second-order Rosenbrock ROS2 method [14]. The method is linearly implicit: to compute the internal stages a system of linear algebraic equations is to be solved.

An illustration of the algae concentration in time is given in Figure 11. The behaviour in time of P, N, C and pH is presented in Figure 12 and Figure 13.

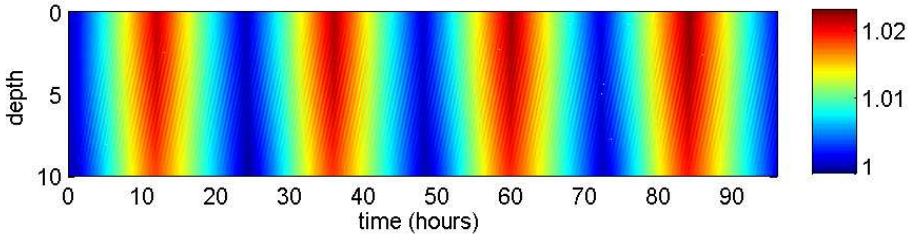

Figure 11: Concentration of algae.

The model equations (19),(27)-(28) are discretized and solved in the domain $z \in [0, z_{max}]$ on the interval $t \in [0, T]$, where $T = 96$ $[hours]$, which corresponds to 4 days. Minerals are being added with a constant rate of $3.64 \cdot 10^{-10}$ $[mol/(l \cdot s)]$ and $2.78 \cdot 10^{-10}$ $[mol/(l \cdot s)]$ for N and P respectively. No carbon dioxide is added. In Figure 11 we notice the periodic nature of the algae concentration. This is due

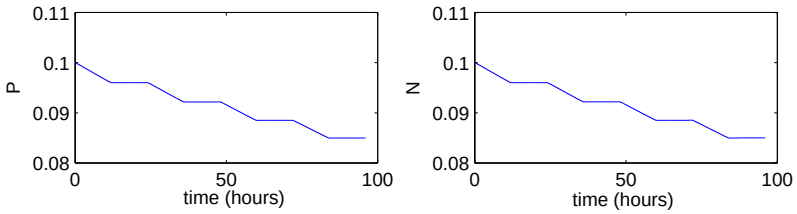

Figure 12: Concentration of P and N.

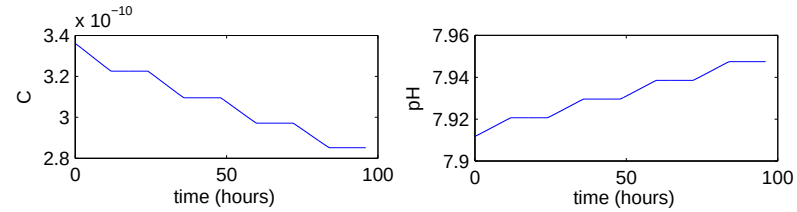

Figure 13: Concentration of C and pH.

to the day-night cycle of the external illumination modeled by $I_0(t)$. The decay of light intensity with depth makes the solution z-dependent. As expected, the algae concentration is lower at the bottom. However, the mixing included in the model diminishes this difference. Due to a large initial concentration of algae, the rate of consumption of minerals is larger than their inflow rate. There is no inflow of carbon dioxide. Thus, the concentration of minerals and of carbon dioxide in the water decreases monotonically as seen from Figure 12 and Figure 13. During one day, the maximum algae concentration is attained in the noon when the light intensity on the surface is the largest. In this particular simulation the value of the maximal concentration increases from day to day at a rate which is comparable with literature data.

4.3 Optimization

We define the average concentration of algae

$$V = \frac{1}{z_{max} T} \int_0^{z_{max}} \int_0^T \mathcal{A}(z,t) dt dz,$$

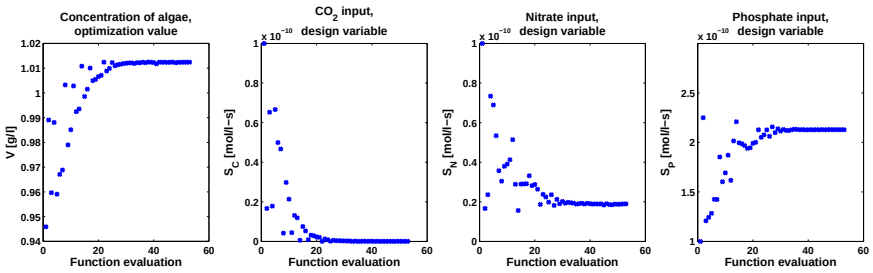

Figure 14: Nelder-Mead simplex optimization.

Table 3: Optimization parameters.

	S_C [mol/(l-s)]	S_N [mol/(l-s)]	S_P [mol/(l-s)]	V [g/l]
Initial	10^{-10}	10^{-10}	10^{-10}	0.946
Optimized	5.309×10^{-14}	1.886×10^{-11}	2.129×10^{-10}	1.0125

or in discrete form

$$V \approx \frac{1}{nm} \sum_{j=1}^{n} \sum_{i=1}^{m} \mathcal{A}(z_i, t_j)\,,$$

where t_i are the time points in which the numerical solution is computed. The average concentration computed by means of the model described above can be optimized as a function of three design variables: carbon dioxide, nitrate and phosphate inflow rates, i.e.

$$\text{maximize } V(S_C, S_N, S_P),$$

$$\text{subject to } S_C \geq 0, S_N \geq 0, S_P \geq 0.$$

For this purpose we apply the Nelder-Mead simplex method [7, 26]. The Nelder-Mead simplex method is designed to find a local optimum of a function. It makes no assumptions about the shape of the function and does not use derivative information. At each iteration the Nelder-Mead simplex method evaluates the function in a finite number of points. In our case one function evaluation corresponds to computing the average concentration of algae.

Figure 14 shows an example of the Nelder-Mead optimization. In this case the optimization required 55 function evaluations. The values of the design variables and correspondingly obtained concentration are plotted for each function evaluation. Table 3 shows the values of the initial guess and the values after optimization.

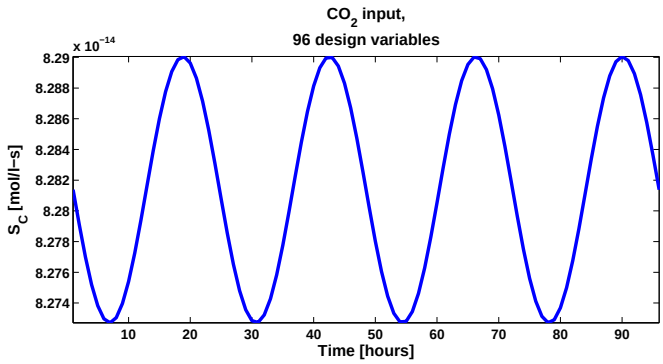

Figure 15: Input of CO_2 as a function of time.

For the optimized values of the design variables the average algae concentration has increased by 7.03%.

Further, the result of the optimization could be improved by assuming S_C, S_N, S_P to be functions of time. Thus, we assume that $\mathbf{s}_C = \{S_{C,i}\}_{i=1}^{L}$, where $S_{C,i}$ is the carbon dioxide inflow rate at time t_i. For fixed S_N and S_P we obtain an optimization problem of L design variables

$$\text{maximize } V(\mathbf{s}_C),$$

$$\text{subject to } S_{C,i} \geq 0.$$

This could result in further improvement of the average algae concentration. As an initial guess for optimization, instead of applying constant carbon dioxide inflow rate, we could use a periodic function with the same period as of the incident light function, with different amplitude and vertical and horizontal shift (see Figure 15).

It is important to note that the average algae concentration function may have multiple maxima. However, the Nelder-Mead simplex method is designed to find a local optimum of a function. It means that initial parameter guess should be close enough to the desirable optimum. For a global optimum other optimization methods (for example, simulated annealing optimization [26]) could be used.

4.4 Conclusions

We proposed a model for the growth of algae in a mineral solution. The model consists of a partial differential equation for the algae concentration coupled to three ordinary differential equations for the phosphate, the nitrate and the carbon dioxide

concentrations. The minerals and the carbon dioxide are assumed to have a constant concentration throughout the volume, while the algae concentration is modeled as a z-dependent quantity. This choice is explained by the strong dependence of light intensity on depth. Moreover, the z-dependency allows us to study the effect of mixing on the algae population. Numerical simulations were performed with the model. To this end, the continuous equations are discretized in space by a finite difference scheme, and the resulting system of ordinary differential equations is integrated in time by a two-stage second-order Rosenbrock method. The simulations have shown a good qualitative prediction for the concentration of algae, minerals and carbon dioxide. In order to achieve also a good quantitative prediction, the parameters of the model have to be adjusted to the experiment. Based on the proposed model, the average concentration of the algae can be optimized by means of derivative-free optimization.

5 Recommendations

In summary, this paper contains the following eight main themes:

1. A review of biological literature, to determine the key factors that effect the growth rate of algae (§1.1).
2. A hierarchical review of existing mathematical models in the literature (§2).
3. Steady-state analysis of one-stage models (§2).
4. A new two-stage model (§3.1).
5. Parameter estimation (§3.2).
6. A new spatial-temporal model of algae growth (§4.1).
7. Numerical solutions of the new models (§3.3 and §4.2).
8. A discussion of how to optimize (§4.3).

Each of these themes represents a step forward in understanding the factors that effect algae growth. All the model extensions proposed (theme 2,3 and 6) can be reduced back to the original model of Huisman *et al* [12] in the correct limit. For example the additional spatial terms introduced in theme 6 can be neglected if the re-mixing rate is small. There will be situations where each, or maybe even all, of these additional effects are important and studying these effects both in isolation and combination will be very enlightening. For the simple models (or the limits

of the more complicated models) the steady-state analysis (theme 3) is very powerful and highlights when these limits are not valid and additional factors need to be included. Estimating the parameters from either the literature (theme 1,5) or by temporal averaging the equations (theme 5) is a challenge that does need more attention; hopefully, new experimental work specifically aimed at determining the control parameters will take place in the next few years. The numerical investigation (theme 7) of the new models is very limited and there is much more scope for numerical studies that allow the simulation of a full algae pond (or maybe even a coupled series of ponds) in the future. Finally, there is room for more work on optimization of the model (theme 8), but early results and a derivative-free method for optimization have been presented.

We have the following recommendations: Construction of a master model including all the effects discussed in §2, §3.1 and §4.1; a detailed analysis on the mathematical limits of this model using the steady-state analysis presented in (§2); further controlled experiment to determine the key parameters; an more detailed investigation of optimisation. The steady-state analysis is useful for two reasons: firstly, it reveals the effect individual factors have on the model; secondly, it gives a very useful test case for any numerical solution of the full system. One of the major problems is a lack of numbers for key parameters in the model §1.1 and §3.2. Therefore a new series of experiments designed to better determine these unknowns would be highly beneficial. Finally, once a good set of parameters is determined, optimization of the model can be undertaken (§4.3) and a detailed investigation (hopefully in collaboration with the industry) of the optimal pond(s) design can be performed.

References

[1] *Private communication with D van der Saar, representative of Phytocare*.

[2] Stichting H2Organic en imares. algencultuur op drainwater uit de bouw. September 2009. *Stichting Innovatie Glastuinbouw Nederland*.

[3] Andersen R. A., editor. *Algal Culturing Techniques*. 2005.

[4] E.L. Brand. The salinity tolerance of forty-six marine phytoplankton isolates. *Estuarine Coastal and Shelf Science*, 18:543–556, 1984.

[5] S. Chen, X. Chen, Y. Peng, and K. Peng. A mathematical model of the effect of nitrogen and phosphorus on the growth of blue-green algae population. *Applied Mathematical Modelling*, 33:1097–1106, 2009.

[6] L.H. Cheng, L. Zhang, and C. J. Chen, H. L.and Gao. Carbon dioxide removal from air by microalgae cultured in a membrane-photobioreacto. *Sep Purif Technol*, 50:324–329, 2006.

[7] A.R. Conn, K. Scheinberg, and L.N. Vicente. Introduction to derivative-free optimization. *MPS-SIAM series on optimization*, 2009.

[8] J. Ramus C.S. Duke, W. Litaker. Effect of temperature on nitrogen-limited growth rate and chemical composition of ulva curvata. *Marine Biology*, 100:143–150, 1989.

[9] R.J. Geider, H. L. MacIntyre, and T. M. Kana. Dynamic model of phytoplankton growth and acclimation: responses of the balanced growth rate and the chlorophyll a:carbon ratio to light, nutrient-limitation and temperature. *Marine Ecology Progress Series*, 148:187–200, 1997.

[10] H. Haario, L. Kalachev, and Laine M. Reduced models of algae growth. *Bulletin of Mathematical Biology*, 71:1626–1648, 2009.

[11] J. Huisman, R.R. Jonker, C. Zonneveld, and F.J. Weissing. Competition for light between phytoplankton species, experimental tests of mechanistic theory. *Ecology*, 80:211–222, 1999.

[12] J. Huisman, H.C.P. Matthijs, P.M. Visser, H. Balke, C.A.M. Signon, J. Passarge, and L.R. Mur. Principles of the light-limited chemostat: theory and ecological applications. *Antonie van Leeuwenhoek*, 81(1-4):117–133, 2002.

[13] J. Huisman, N.N. Pham Thi, D.M. Karl, and B. Sommeijer. Reduced mixing generates oscillations and chaos in the oceanic deep chlorophyll maximum. *Nature*, 439:322–325, 2006.

[14] W. Hundsdorfer and J.G. Verwer. Numerical solution of time-dependent advection-diffusion-reaction equations. *Springer Series in Comp. Math.*, 33, 2003.

[15] E. Kebede-Westhead, C. Pizarro, and W. W. Mulbry. Treatment of swine manure effluent using freshwater algae: Production, nutrient recovery, and elemental composition of algal biomass at four effluent loading rates. *Journal of Applied Phycology*, 18:41–46, 2006.

[16] C.A. Klausmeier, E. Litchman, T. Daufresne, and S.A. Levin. Phytoplankton stoichiometry. *Ecol. Res.*, 23:479–485, 2008.

[17] C.A. Klausmeier, E. Litchman, and S.A. Levin. Phytoplankton growth and stoichiometry under multiple nutrient limitation. *Limnol Oceanogr.*, (4):1463–1470, 2004.

[18] de Leenheer, P., S.A. Levin, E.D. Sontag, and C.A. Klausmeier. Global stability in a chemostat with multiple nutrients. *J. Math. Biol.*, 52:419–438, 2006.

[19] B. Li and H.L. Smith. Global dynamics of microbial competition for two resources with internal storage. *J. Math. Biol.*, 55:481–515, 2007.

[20] J.C. Merchuk. Photobioreactor design and fluid dynamics. *Chem. Biochem. Eng. Q.*, 21(4):345–355, 2007.

[21] Víctor J. Nuñez, Domenico Voltolina, Mario Nieves, Pablo Piña, Alejandra Medina, and Martín Guerrero. Nitrogen budget in scenedesmus obliquus cultures with artificial wastewater. *Bioresource Technology*, 78(2):161 – 164, 2001.

[22] Erik Olson. The krib: Aquaria and tropical fish. `http://www.thekrib.com/Plants/CO2/kh-ph-co2-chart.html` .

[23] Erik Olson. The krib: Aquaria and tropical fish. `http://www.thekrib.com/Plants/Tech/intensorama.html` .

[24] E. Paasche. Biology and physiology of coccolithophorids. *Annual Review of Microbiology*, 22:71–86, 1968.

[25] N.N. Pham Thi. Numerical analysis of phytoplankton dynamics. PhD thesis, University of Amsterdam, 2006.

[26] H. Press, W, S.A. Teukolsky, and W.T. Vetterling. Numerical recipes: the art of scientific computing. 2007.

[27] O. Pulz. Photobioreactors: production systems for phototrophic microorganisms. *Appl Microbiol Biotechnol*, 57:287–293, 2001.

[28] G.Y. Rhee. Effects of $n : p$ atomic ratios and nitrate limitation on algal growth, cell composition, and nitrate uptake. *Limnol. Oceanogr.*, 23:10–25, 1978.

[29] G.Y. Rhee. Continous culture in phytoplankton ecology. *Adv. in Aquatic Microbiology*, pages 151–203, 1980.

[30] Dénis van Rensburg. The chemistry in shadehouses. http://www.ont.co.za/new_page_1.htm .

[31] A. Vonshak. Spirulina platensis (arthrospira): Physiology, cell biology and biotechnology. *Journal of Applied Phycology*, 9(3), 1997.

PREVIOUS PUBLICATIONS IN THIS SERIES:

Number	Author(s)	Title	Month
10-55	Q.Z. Hou A.S. Tijsseling R.M.M. Mattheij	An improvement for singularity in 2-D corrective smoothed particle method with application to Poisson problem	Sept. '10
10-56	L.J. Astola L.M.J. Florack	Finsler geometry on higher order tensor fields and applications to high angular resolution diffusion imaging	Sept. '10
10-57	L.J. Astola A. Fuster L.M.J. Florack	A Riemannian scalar measure for diffusion tensor images	Sept. '10
10-58	J.H.M. ten Thije Boonkkamp J. van Dijk L. Liu K.S.C. Peerenboom	The finite volume-complete flux scheme for one-dimensional advection-diffusion-reaction systems	Oct. '10
10-59	A. Thornton T. Weinhart O. Bokhove B. Zhang D.M. van der Sar K. Kumar M. Pisarenco M. Rudnaya V. Savcenco J. Rademacher J. Zijlstra A. Szabelska J. Zyprych M. van der Schans V. Timperio F. Veerman	Modeling and optimization of algae growth	Oct. '10

Ontwerp: de Tantes,
Tobias Baanders, CWI